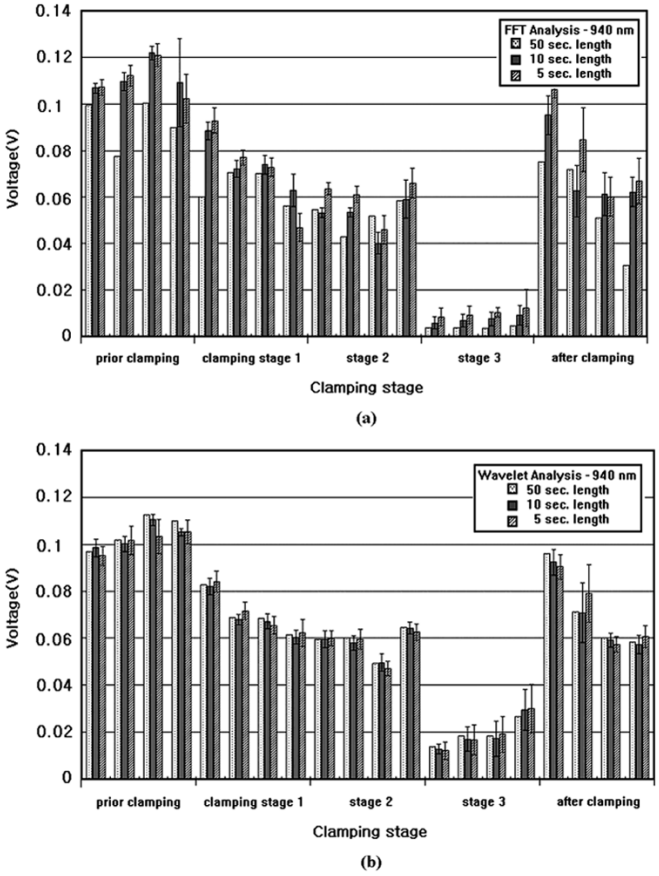

Fig. 3. The results from FFT and DWT analysis for the *in vivo* data showing 940 nm wavelengths. Note that for the DWT analysis of (b) there is very little difference in the 50-, 10-, and 5–s data while for the FFT analysis depicted in (a) the intensity fluctuates wildly depending on the window size. The average drops and then recovers as expected for the perfusion signal as the vessels are clamped and then released. The error bars indicate standard deviation.

IV. Conclusion

In this study the potential of wavelet analysis for amplitude estimation of perfusion signals *in vitro* and *in vivo* was explored. It was found that FFT and wavelet analysis gave very similar results on periodic perfusion signals present in the *in vitro* study. However through analysis of *in vivo* data, which contains quasi-periodic perfusion signals, wavelet analysis had a lower standard deviation and greater stability than the FFT. The wavelet analysis was able to maintain steady peak height estimations throughout all file lengths down to 5 s. This significant reduction in data size is critical in implantable applications where achieving minimal power consumption is paramount. Overall it has been shown that wavelet analysis is a reasonable method for analysis of perfusion data using an oximetry approach and has proven to be more effective than FFT for this quasi-periodic *in vivo* data.

References

[1] J. Pumprla *et al.*, "Functional assessment of heart rate variability: Physiological basis and practical applications," *Int. J. Cardiol.*, vol. 84, pp. 1–14, 2002.

[2] L. S. Costanzo, *Physiology*. Philadelphia, PA: Saunders, 1998.

[3] J. Enderle *et al.*, *Introduction to Biomedical Engineering*. New York: Academic, 1999.

[4] K. K. Rusch, R. Sankar, and J. E. Scharf, "Signal processing methods for pulse oximetry," *Comput. Biol. Med.*, vol. 26–2, pp. 143–159, 1996.

[5] J. G. Webster, *Design of Pulse Oximeters*. Philadelphia, PA: Inst. Phys., 1997.

[6] A. Stefanovska, M. Bracic, and H. Kvernmo, "Wavelet analysis of oscillations in the peripheral blood circulation measured by laser Doppler technique," *IEEE Trans. Biomed. Eng.*, vol. 46, no. 10, pp. 1230–1239, Oct. 1999.

[7] B. Dixon *et al.*, "Monte Carlo modeling for perfusion monitoring," in *Proc. SPIE Photonics West Conf.*, vol. 4965–06, 2003.

[8] M. N. Ericson *et al.*, "*In vivo* application of a minimally invasive oximeter based perfusion sensor," in *Proc. 2nd Joint IEEE EMBS/BMES Conf.*, vol. 3, 2002, pp. 1789–1790.

[9] A. Rakotomamonjy, D. Coast, and P. Marché, "Wavelet-based enhancement of the signal-averaged ECG for late potentials detection," *Med. Bio. Eng. Comput.*, vol. 37, pp. 750–759, 1999.

[10] I. Daubechies, *Ten lectures on wavelets*. Philadelphia, PA: Soc. Ind. Appl. Math., 1992.

Automatic Grading of Retinal Vessel Caliber

Huiqi Li, Wynne Hsu, Mong Li Lee*, and Tien Yin Wong

***Abstract*—New clinical studies suggest that narrowing of the retinal blood vessels may be an early indicator of cardiovascular diseases. One measure to quantify the severity of retinal arteriolar narrowing is the arteriolar-to-venular diameter ratio (AVR). The manual computation of AVR is a tedious process involving repeated measurements of the diameters of all arterioles and venules in the retinal images by human graders. Consistency and reproducibility are concerns. To facilitate large-scale clinical use in the general population, it is essential to have a precise, efficient and automatic system to compute this AVR. This paper describes a new approach to obtain AVR. The starting points of vessels are detected using a matched Gaussian filter. The detected vessels are traced with the help of a combined Kalman filter and Gaussian filter. A modified Gaussian model that takes into account the central light reflection of arterioles is proposed to describe the vessel profile. The width of a vessel is obtained by data fitting. Experimental results indicate a 97.1% success rate in the identification of vessel starting points, and a 99.2% success rate in the tracking of retinal vessels. The accuracy of the AVR computation is well within the acceptable range of deviation among the human graders, with a mean relative AVR error of 4.4%. The system has interested clinical research groups worldwide and will be tested in clinical studies.**

***Index Terms*—AVR, cardiovascular disease, retinal image, vessel measurement, vessel modeling.**

I. Introduction

Cardiovascular diseases such as stroke and coronary heart disease are the leading causes of morbidity and mortality worldwide [1]. New studies show that an early marker of cardiovascular risk is generalized narrowing of the retinal blood vessels [2]. A measurement that has been used to quantify the degree of narrowing is the arteriolar-to-venular diameter ratio (AVR) [3]. This AVR ratio is determined by measuring the diameters of individual retinal arteriolar and venular calibers. A

Manuscript received April 1, 2004; revised December 5, 2004. *Asterisk indicates corresponding author.*

H. Li is with the Institute for Infocomm Research, Singapore, Singapore (huiqili@i2r.a-star.edu.sg).

W. Hsu is with the School of Computing, National University of Singapore, Singapore 117543, Singapore (e-mail: whsu@comp.nus.edu.sg).

*M. L. Lee is with the School of Computing, National University of Singapore, Singapore 117543, Singapore (leeml@comp.nus.edu.sg).

T. Y. Wong is with the Department of Ophthalmology, National University of Singapore, Singapore 117543, Singapore (ophwty@nus.edu.sg).

Digital Object Identifier 10.1109/TBME.2005.847402

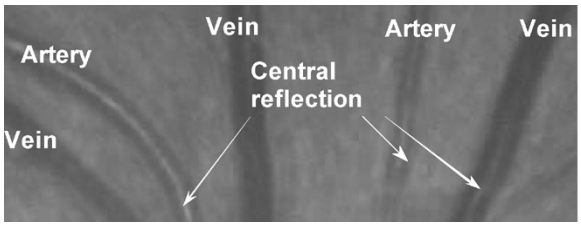

Fig. 1. Central light reflection is observed in blood vessels. (The reflection is indicated by the arrows.)

lower AVR is associated with higher blood pressures, and increased risk of stroke, diabetes, and hypertension.

The current process of calculating the AVR ratio by measuring retinal vessel diameters from retinal photographic images is tedious and highly operator-dependent. A human grader must first determine the vessel type (arteriole or venule). The diameter of each vessel is then measured manually. This process is not only time-consuming, but it varies from one inspection to the next even when the same human grader is involved. Hence, reproducibility is a major concern [4]. An average human grader typically needs to spend up to twenty minutes per retinal image to complete the measurement. This is certainly not feasible for large-scale research studies and clinical utility. Clearly, there is a need for a more precise and efficient system that can grade the retinal vessels automatically.

Existing techniques for vessel detection in retinal images can be broadly classified into two categories: scanning methods [5] and tracking methods [6]. Scanning methods require a two-step processing of each image pixel: enhancement and thresholding. An additional tracking step is needed if the application requires that the vessel structure be identified. In contrast, the tracking approach utilizes local image properties to trace the vessels from initial points. This approach is faster since it only processes the pixels close to the vessels. The proposed system adopts the tracking strategy since it can provide a meaningful description of the vessel structure and is computationally efficient.

The scanning and tracking strategies are based on either the vessel boundary detection or the vessel body extraction. In boundary detection, vessel edges are detected by edge detectors [7], morphological methods [8], or deformable models [9]. Edge fitting that minimizes the distance between the original data and a predefined model is utilized in the vessel body extraction [5], [10]. It is more robust since it extracts the vessel as a whole.

Various models have been designed for profiling blood vessels: regular [11], triangular [12], Elliptical [13], and Gaussian [5], [14]. However, all these models do not consider the central light reflection in the vessels [15]. Fig. 1 shows the light reflection in blood vessels (indicated by arrows). It is important for a model to take into account this light reflection in order not to miss these vessels.

This paper describes a new approach to obtain the AVR. The starting points of vessels are detected using a matched Gaussian filter. The detected vessels are traced with the help of a combined Kalman filter and Gaussian filter. A modified Gaussian model that considers the central light reflection is developed to describe the vessel profile. The width of a vessel is obtained by data fitting. Experimental results indicate a 97.1% success rate in the identification of vessel starting points, and a 99.2% success rate in the tracking of retinal vessels. The accuracy of the AVR computation, with a mean relative AVR error of 4.4%, is well within the acceptable range of deviation among the human graders.

II. Methodology

A. Measurement of Vessel Diameters

The tracking strategy first identifies the starting points of all vessels near the optic disc. These vessels are tracked outwards toward the peripheral of the retinal image. In order to identify the starting points for tracking the retina vessels, we restrict the area of interests to Zone B, which is defined as the region from 1/2 an optic disc diameter to 1 optic disc diameter from the disc margin. We model the vessels as consisting of piecewise linear segments of second-order derivative Gaussian filter. This allows us to track along the orientation of a vessel. The matched filters with different rotations are then convolved with the intensity profile on the inner circle of Zone B. The highest response among all the rotations is defined as the convolution response of that point. The local maxima of the convolution response on the profile are selected as the starting points of the vessels.

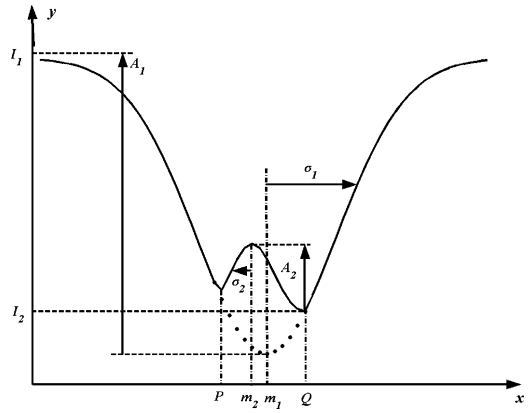

Fig. 2. Modified Gaussian model. A_1, m_1, σ_1, A_1, m_1, and σ_2 indicate the height, peak position and width distribution of the Gaussian function for vessel trunk and for central reflection, respectively.

Next, the vessels are tracked from the detected starting points using Kalman estimation [11] and matched Gaussian filtering. In order to obtain an accurate measurement of vessel width during the tracking of vessels, we note that there is a dip at the bottom of many vessel profiles. This is caused by the light reflection at the back of the vessel, also known as the central reflection problem. We design a new model to describe the vessel profile, taking the central reflection into account

$$y = f(x) = \begin{cases} -A_1 e^{-\frac{(x-m_1)^2}{2\sigma_1^2}} + I_1 & x < P, x > Q \\ A_2 e^{-\frac{(x-m_2)^2}{2\sigma_2^2}} + I_2 & P \le x \le Q \end{cases} \quad (1)$$

where A_1 represents the height of the Gaussian, m_1 is the position of peak, and σ_1 indicates the width of Gaussian function. I_1 is the intensity of the immediate retinal background; A_2, m_2 and σ_2 indicate the height, peak position and width distribution of the central reflection, respectively; P and Q are the positions of the left and right minimum in the intensity on the profile respectively; I_2 represents the minimum intensity.

The proposed modified Gaussian model is shown in Fig. 2. We can now fit the normal profile of a tracked vessel to the model. The difference between the model and the vessel profile is known as fitting error or residual error. The fitting of the vessel to the model proceeds iteratively, to estimate the values of the parameters in the model that minimize the residue error. We adopt the Marquardt method [16] to obtain the optimum parameter values. Once the vessel profile has been fitted to a modified Gaussian model, the vessel width can be decided by σ_1 as studies have shown that there is a linear relationship between σ_1 and vessel width [14].

B. Calculation of AVR

Currently, our system has a manual function to input and validate the vessel type: artery or vein. The AVR is calculated according to the Wisconsin protocol [3]. Two measures, the Central Retinal Artery Equiva-

TABLE I
RESULTS OF STARTING POINT DETECTION

	Large Vessels	Small Vessels
Total Number	375	260
Automatic Detection	364	140
Success Rate	97.1%	53.8%

TABLE II
RESULTS OF VESSEL TRACKING

	Vessels
Total Number	375
Track Not Started	2
Not Full Track	1
Success Rate	99.2%

lent (CRAE) and Central Retinal Vein Equivalent (CRVE) are defined. The formula for CRAE is described as the following:

$$W_c = \left(0.87W_a^2 + 1.01W_b^2 - 0.22W_aW_b - 10.76\right)^{\frac{1}{2}} \quad (2)$$

where W_c is the width of the trunk arteriole, W_a is the width of the small branch, and W_b is the width of the large branch. The CRVE is calculated as follows:

$$W_c = \left(0.72W_a^2 + 0.91W_b^2 + 450.05\right)^{\frac{1}{2}} \quad (3)$$

where W_c is the width of the trunk vein, W_a is the width of the small branch, and W_b is the width of the large branch. With that, we can compute the AVR ratio as follows:

$$\text{AVR} = \frac{\text{CRAE}}{\text{CRVE}}. \quad (4)$$

III. EXPERIMENT STUDY WITH RESULTS

A user-friendly system has been developed using Visual C++ to measure AVR in retinal images. Thirty-five retinal images obtained from a population-based study in Wisconsin are tested by the software system. These color retinal images are captured from the digital retinal camera system, which includes a Canon CR6-45NM nonmydriatic retinal camera and a Canon EOS D60 digital camera. The images are saved in the format of 24-bit Bitmap with the resolution of 3072 × 2048 pixels. In these images, one pixel stands for 5.33 μm.

Experimental results of the accuracy of starting points detection is shown in Table I. Large vessels are defined as those vessels whose diameters are more than 45 μm. Those vessels with diameters less than 45 μm are defined as small vessels, and can be ignored in the AVR calculation [3]. We observe that 97.1% of the large vessels' starting points have been identified correctly using the matched Gaussian filter. For those vessels whose starting points are missed, our system allows the manual input by human graders.

Once the starting points have been identified, we track the vessels using a combined Kalman filter and Gaussian filter within Zone B. Table II summarizes the tracking results. Vessel tracking is considered successful if the whole vessel trace in Zone B is detected before any branching point. In our experiments, the success rate is 99.2%.

Next, 505 vessel segments are obtained from the thirty-five images to study the modified Gaussian model. Fig. 3 gives the performance of the modified Gaussian model and the standard Gaussian model. The residual errors are averaged for the same σ_1 (round to regular) obtained. It is noted that the performance of the two models is similar when the vessel is small (σ_1 is small). However, the residual error is much larger in the standard Gaussian model than in the modified Gaussian mode when σ_1 becomes larger. Therefore, we conclude that the proposed modified Gaussian model is more accurate for the vessel profile in the retinal images especially for the large vessels.

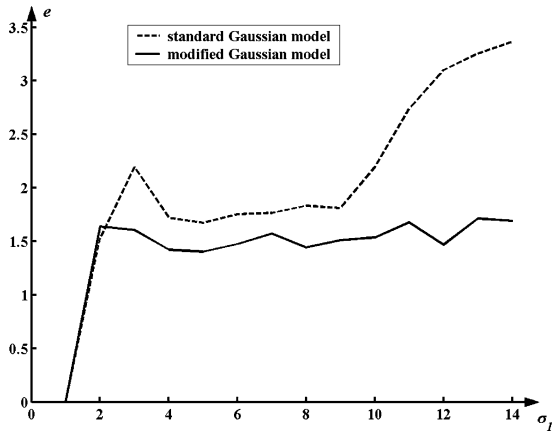

Fig. 3. Comparison of the two models. The residual error e is similar when σ_1 is small. However, it is much larger in the standard Gaussian model than in the modified Gaussian mode when σ_1 becomes larger.

TABLE III
RESULTS OF AVR COMPUTATION

Artery	Grader result	System result	Vein	Grader result	System result
A1	77.1	76.0	**V1**	151.2	145.8
A2	85.8	77.7	**V2**	91.2	94.3
A3	55.5	48.8	**V3**	89.1	82.1
A4	71.4	65.7	**V4**	126.6	130.0
A5	76.8	73.6	**V5**	52.5	57.4
A6	109.2	108.9			
A7	60.0	61.4			
A8	88.8	83.9			
CRAE	181.6	179.2	**CRVE**	201.2	203.6
AVR	0.90	0.88			

In our final set of experiments, we evaluate the accuracy of the computed CRAE, CRVE, and AVR as compared to the human graders. Thirty-five color retinal images are tested. An example is shown in Table III. The mean relative errors of the 35 images for CRAE, CRVE and AVR are 4.5%, 3.2% and 4.4%, respectively. This is well within the acceptable range of deviation among the human graders [17].

IV. CONCLUSION

In this paper, we have proposed a new approach for the automatic grading of retinal vessel caliber. We have investigated robust methods to detect the starting points of vessels, track the vessels, and determine the vessel width. A modified Gaussian model is proposed to describe the vessel profile. The individual vessel diameter is calculated to obtain the summary variables CRAE, CRVE and AVR. Experimental results indicate a 97.1% success rate in the identification of vessel starting points, and a 99.2% success rate in the tracking of retinal vessels. The accuracy of the AVR computation is consistent with the human graders, with a mean relative AVR error of 4.4%. To date, many clinical research groups have shown interests in using the proposed system for cardiovascular risk prediction in research studies. Further research will confirm its ease of use in clinical settings.

REFERENCES

[1] National heart lung and blood institute, The Morbidity and Mortality: Chartbook on Cardiovascular, Lung and Blood Diseases, US Department of Health and Human Services, National Institute of Health, Bathesda, MD, 1998.

[2] T. Y. Wong, R. Klein, B. E. K. Klein, and J. M. Tielsch *et al.*, "Retinal microvascular abnormalities, and their relation to hypertension, cardiovascular diseases and mortality," *Survey Ophthalmol.*, vol. 46, pp. 59–80, 2001.

[3] L. D. Hubbard and R. J. Brothers *et al.*, "Methods for evaluation of retinal microvascular abnormalities associated with hypertension/sclerosis in the atherosclerosis risk in communities studies," *Ophthalmology*, vol. 106, pp. 2269–2280, 1999.

[4] T. Y. Wong, L. D. Hubbard, and R. Klein *et al.*, "Retinal microvascular abnormalities and blood pressure in older people: the cardiovascular health study," *Br. J. Ophthalmol.*, vol. 82, pp. 1007–1013, 2002.

[5] A. Hoover, V. Kouznetsova, and M. Goldbaum, "Locating blood vessels in retinal images by piecewise threshold probing of a matched filter response," *IEEE Trans. Med. Imag.*, vol. 19, no. 3, pp. 203–210, Mar. 2000.

[6] Y. A. Tolias and S. M. Panas, "A fuzzy vessel tracking algorithm for retinal images based on fuzzy clustering," *IEEE Trans. Med. Imag.*, vol. 17, no. 2, pp. 263–273, Apr. 1998.

[7] M. Lalonde, L. Gagnon, and M. C. Boucher, "Non-recursive paired tracking for vessel extraction from retinal images," in *Conf. Vision Interface*, 2000, pp. 61–68.

[8] R. M. Haralick, S. R. Sternberg, and X. Zhuang, "Image analysis using mathematical morphology," *IEEE Trans. Pattern Anal. Mach. Intell.*, vol. PAMI-9, pp. 532–550, 1987.

[9] T. McInerney and D. Terzopoulos, "Deformable models in medical image analysis: a survey," *Med. Image Anal.*, vol. 1, no. 2, pp. 91–108, 1996.

[10] M. Goldbaum, S. Moezzi, A. Taylor, and S. Chatterjee *et al.*, "Automated diagnosis and image understanding with object extraction, object classification, and inferencing in retinal images," in *Proc. IEEE Int. Conf. Image Processing*, vol. 3, 1996, pp. 695–698.

[11] O. Chutatape, Z. Liu, and S. M. Krishnan, "Retinal blood vessel detection and tracking by matched Gaussian and Kalman filters," in *Proc. 20th Annu. Conf. IEEE Eng. Med. Biol. Soc.* ., 1998, pp. 3144–3148.

[12] I. Liu and Y. Sun, "Recursive tracking of vascular networks in angiograms based on the detection-deletion scheme," *IEEE Trans. Med. Imag.*, vol. 12, no. 2, pp. 334–341, Apr. 1993.

[13] P. Jasiobedzki, C. J. Taylor, and J. N. H. Brunt, "Automated analysis of retinal images," *Image Vision Computing*, vol. 11, no. 3, pp. 139–144, 1993.

[14] G. Luo, O. Chutatape, and S. M. Krishnan, "Detection and measurement of retinal vessels in fundus images using amplitude modified second-order Gaussian filter," *IEEE Tran. Biomed. Eng.*, vol. 49, no. 2, pp. 168–172, Feb. 2002.

[15] W. H. Spencer, *Ophthalmic Pathology: An Atlas and Textbook*. Philadelphia, PA: Saunders, 1996.

[16] W. H. Press, S. A. Teukolsky, W. T. Vetterling, and B. P. Flannery, *Numerical Recipes in C: the Art of Scientific Computing*. Cambridge, U.K.: Cambridge Univ. Press, 1993.

[17] D. J. Couper, R. Klein, L. D. Hubbard, and T. Y. Wong *et al.*, "Reliability of retinal photography in the assessment of retinal microvascular characteristics: the atherosclerosis risk in the communities study," *Am. J. Ophthalmol.*, vol. 133, pp. 78–88, 2002.

An Autocorrelation-Based Time Domain Analysis Technique for Monitoring Perfusion and Oxygenation in Transplanted Organs

Hariharan Subramanian, Bennett L. Ibey, Weijian Xu, Mark A. Wilson, M. Nance Ericson, and Gerard L. Coté*

***Abstract*—In designing an implantable sensor for perfusion monitoring of transplant organs the ability of the sensor to gather perfusion information with limited power consumption and in near real time is paramount. The following work was performed to provide a processing method that is able to predict perfusion and oxygenation change within the blood flowing through a transplanted organ. For this application, an autocorrelation-based algorithm was used to reduce the acquisition time required for fast Fourier transform (FFT) analysis while retaining the accuracy inherent to FFT analysis. In order to provide data proving that the developed method is able to predict perfusion as accurately as FFT two experiments were developed isolating both periodic and quasi-periodic cardiac frequencies. It was shown that the autocorrelation-based method was able to perform comparably with FFT (limited to a sampling frequency of 300 Hz) and maintain accuracy down to acquisition times as low as 4 s in length.**

***Index Terms*—Autocorrelation, FFT, perfusion, transplant, pulse oximeter.**

I. INTRODUCTION

In 2002, over 24 000 patients received transplanted organs such as liver, kidney, and intestines in the United States [1]. One parameter of interest in the transplant procedure is a measure of local blood perfusion and oxygenation within the graft. Prolonged and untreated loss of blood perfusion due to acute rejection or mechanical failure (sutures) will result in loss of organ function and be hazardous to the transplant patient [2]. The week following transplant proves the most critical because of high immune response and healing within the organ. Being able to measure the local blood perfusion within a transplanted organ continuously within this crucial period will allow physicians to diagnose organ failure earlier and potentially increase patient and graft survival after surgery [2].

In order to obtain the local blood perfusion information, an *in vivo* sensor to detect the blood perfusion and oxygenation following organ transplant is being developed by the Optical Biosensing Laboratory at Texas A&M University in collaboration with Oak Ridge National Laboratory and the University of Pittsburgh Medical School [3]. The sensor is based on a modified pulse-oximeter that can be implanted onto the transplant organ during the surgical procedure and remain in the body throughout the recovery period. The signal is sent from the sensor to

Manuscript received January 12, 2004; revised December 23, 2004. This paper was supported of the U.S. Department of Energy, Contract no. DE-AC05-00OR22725. *Asterisk indicates corresponding author.*

H. Subramanian and B. L. Ibey are with the Department of Biomedical Engineering, Texas A&M University, College Station, TX 77843-3120 USA (e-mail: hariharan@tamu.edu; bli6339@tamu.edu).

W. Xu is with the Department of Surgery, University of Pittsburgh, Pittsburgh, PA 15213 USA (e-mail: xuw@msx.upmc.edu).

M. A. Wilson is with the Department of Surgery, University of Pittsburgh, Pittsburgh, PA 15240 USA; (e-mail: Mark.wilson5@med.va.gov).

M. N. Ericson is with the Oak Ridge National Laboratory, Oak Ridge, TN 37831 USA (e-mail: ericsonmn@ornl.gov).

*G. L. Coté is with the Department of Biomedical Engineering, Texas A&M University, Mail Stop 3120, College Station, TX 77843-3120 USA (e-mail: gcote@tamu.edu).

Digital Object Identifier 10.1109/TBME.2005.847552